9-25-2020

Progress Report III: Fabrication of Nanopores in Silicon Nitride Membranes using Electron-beam Lithography

Mingxuan Ma
Singh Center for Nanotechnology, mxma@seas.upenn.edu

Hiromichi Yamamoto
Singh Center for Nanotechnology, hyam@seas.upenn.edu

Progress Report III: Fabrication of Nanopores in Silicon Nitride Membranes using Electron-beam Lithography

Abstract

This report describes the fabrication of a long-range orderly nanopore structure in free-standing siliconnitride membranes using electron-beam lithography (EBL). The parameter setting and challenges of eachstep are discussed.

Keywords

Nanopore, Electron-beam Lithography, Silicon Nitride

Disciplines

Engineering | Physical Sciences and Mathematics

Progress Report III: Fabrication of Nanopores in Silicon Nitride Membranes using Electron-beam Lithography

Mingxuan Ma and Hiromichi Yamamoto[1, a)]
[1]*Singh Center for Nanotechnology, University of Pennsylvania*
3205 Walnut St. Philadelphia, PA 19104

(Dated: Received 21 September 2020; accepted 25 September 2020)

This report describes the fabrication of a long-range orderly nanopore structure in free-standing silicon nitride membranes using electron-beam lithography (EBL). The parameter setting and challenges of each step are discussed.

Key Words: Nanopore, Electron-beam Lithography, Silicon Nitride

I. Introduction

Since first being designed by David Deamer in 1989, nanopores have been explored for applications in various fields, such as drug delivery,[1] organic solar cells,[2] next-generation DNA sequencing tools,[3] field-effect transistors,[4] and optical detection.[5] Compared with their biological counterparts, solid-state nanopores exhibit adjustable pore dimensions and uniformity, mechanically and chemically robustness and process compatibility, which promise them to be a powerful platform for future devices.[6] As a research hotspot, different techniques have been developed for constructing nanopore structures, as can be divided into maskless methods and template-assisted methods. However, fabrication of a long-range orderly nanopore structure with multi-step size control remains a challenge.

The goal of this project is to fabricate ∼5 nm diameter nanopores in a silicon nitride membrane, in order to meet potential demand from many applications. We previously reported preparation of a membrane of a layered structure of 36.8 µm thick Si and 116 nm thick silicon nitride.[7] Furthermore, we reported preparation of a nanopore film using the self-assembly of PS-b-PMMA film, and showed nanopore transfer from the block copolymer (BCP) film to the Si substrate through a hard mask of aluminum oxide.[8] Here, we describe a progress report of fabrication of a 300 µm x 300 µm size array of nanopores in silicon nitride membrane using e-beam lithography, and shrinkage of nanopores using Atomic Layer Deposition (ALD) of aluminum oxide, as shown in FIG. 1.

II. Experiment

A. Silicon nitride deposition

A (100) Si double side polished wafer was cleaned using the RCA cleaning. Then the 250 nm thick silicon nitride films were deposited on both sides of the Si wafer, using Low Pressure Chemical Vapor Deposition (LPCVD) for 1 hour. The thickness of the silicon nitride films was determined using Filmetrics F50 after the deposition.

B. Photo-lithography

Side 1 was spin-coated with S1813 photoresist at 4000 rpm for 60 seconds, followed by baking at 115°C for 5 minutes on a hot plate. The wafer was then exposed to 405 nm UV light using SUSS MicroTec MA6 Gen3 Mask Aligner with an exposure dose of 150 mJ/cm^2. After the exposure, the wafer was developed in AZ-300 (Microchem) for 1 minute and then rinsed in DI water.

C. Reactive ion etching of Side 1

The silicon nitride film on side 1 was dry etched through the developed photoresist, using Oxford 80 plus reactive ion etching (RIE) with the following condition: O_2 = 10 sccm, SF_6 = 50 sccm, pressure = 150 mTorr, power = 100W, T = 15°C . The etching rate is estimated to be 50.6 nm/min. The whole time for the 250 nm film is 5 minutes. The wafer's edge needs to be covered with Kapton tape to prevent silicon nitride on the other side from being etched during this process. Then the photoresist was stripped with sonication in acetone for 30 seconds. The thickness of the window was measured by a KLA Tencor P7 2D Profilometer.

D. Protective coating on Side 2

To protect the silicon nitride layer on Side 2 from KOH wet etching, Protek B3 Primer was spin coated at 1500 RPM for 1 min on Side 2, followed by baking at 200°C for 60 seconds on a hot plate to harden the primer. Protek B3 was spin coated at 1000 RPM for 60 seconds on top of the primer layer, followed by baking at 115°C for 2 min. The wafer was again baked at 250°C for 50 seconds to strengthen the bonding between Protek B3 primer and Protek B3 and between the entire coating and the silicon nitride layer.

a)Electronic mail: hyam@seas.upenn.edu

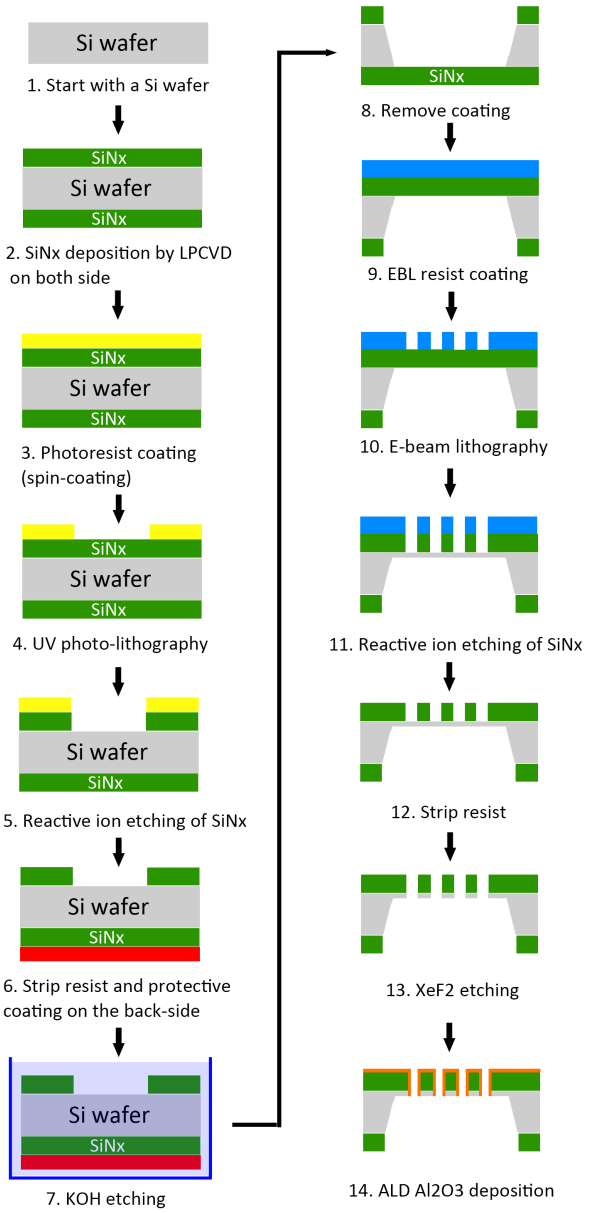

FIG. 1: Process flow (Fabrication of free-standing silicon nitride membrane and nanopore arrays included in this report)

E. KOH etching of silicon on Side 1

The Si exposed through the silicon nitride hard mask window was wet etched using a 30 wt% KOH solution at 75°C. The wet etching was carried out for 5 hours. The Si thickness of 450 µm was etched by wet-etch on Side 1. Then the protective coating was removed by 49wt% HF solution for 1 min. The thickness of the window was measured by Zygo NewView 7300 Optical Profilometer.

F. Electron-beam lithography

A 186 nm thick ZEP-520A (dissolved in anisole (v/v = 1/1)) film was spin coated at 1500 rpm for 60 seconds, followed by baking at 180°C for 5 minutes on a hot plate to minimize any defects. Then, to prevent the insulating silicon nitride and the resist film from charging due to e-beam, DisCharge DI was spin coated at 2000 rpm for 60 seconds.[9] No pre-bake is required and the chip need to cool down to the room temperature for 5 min. Elionix ELS-7500EX was used for e-beam lithography with the following condition: an accelerating voltage of 50 kV; a beam current of 100 pA; an objective lens aperture of 40 µm; the e-beam dose = 200 µC/cm^2 in the area of 300x300 µm^2 with the total dots of 60000x60000; the dose time of 0.5 µsec. The ZEP520A film exposes was developed in O-xylene for 70 seconds and rinsed in 2-propanol for 30 seconds.

TABLE I: Gap depth measured by 2D Profilometer after 1^{st} reactive ion etching

No.	Time (s)	Depth (nm)
1	50	42.2
2	300	1463
3	370	1920

G. Reactive ion etching of Side 2

The pattern fabricated by electron beam lithography was transferred into the silicon nitride membrane by another step of reactive ion etching with the following condition: CF_4 = 20 sccm, pressure = 150 mTorr, power = 100W, T = 15°C. The etching time is 3 minutes. After RIE, the remaining resists were removed via oxygen (O_2) plasma etching for 2 minute and then, the substrate was washed with acetone and isopropyl alcohol (IPA) for 3 minutes, respectively.[10]

III. Results and Discussion

A. Reactive ion etching

To fabricate the window structure, the 1^{st} RIE needs to remove all the exposed silicon nitride on side 1, as shown in FIG.1. Sulfur hexafluoride (SF_6) plasma has a relatively high etch rate of silicon nitride and bulk silicon. RIE of SF_6 etched the upper layer of silicon nitride, then etched the silicon at a higher rate. TABLE I indicates that the etch rate of silicon nitride is 0.844 nm/s, and the etch rate of silicon is 6.52 nm/s. To ensure that silicon nitride is wholly etched, part of silicon was sacrificed, as the etching time was set to be 4 minutes.

The 2^{nd} RIE is to transfer the EBL pattern to the silicon nitride layer. Before this step, two different kinds of commonly used electron-sensitive resist, PMMA and ZEP520A, have been examined. Since the fabrication of nanopores has a high requirement for resolution, the resist's choice shows a significant impact on the final pattern. ZEP520A and PMMA were compared experimentally via etching rate measurement and predicted theoretically using their Ohnishi Numbers (O.N.). The O.N. of a specific resist can be calculated using the following equation as O.N. = N / (N_c - N_0), where N stands for the

TABLE II: The etching rates and Ohnishi parameters of ZEP520A and PMMA along with corresponding ratios.

Resist	Etching rate (nm/s)	Ohnishi parameter
PMMA	1.23	5
ZEP520A	0.85	2.82
Ratio	1.45	1.77

number of atoms in one monomer, N_c stands for the number of carbon atoms in one monomer, and N_0 stands for the number of oxygen atoms in one monomer.[11] TABLE II indicates the etching rates of PMMA and ZEP520A along with their corresponding Ohnishi parameters for comparison.

The data in TABLE II corroborated with what was predicted by Ohnishi Parameters: PMMA, which had a higher Ohnishi Parameter, indeed had a higher etching rate than ZEP520A. Thus, ZEP520A was a better resist of CF_4 plasma etching. The Ohnishi parameter's accuracy was evaluated by comparing the ratio between experimental etching rates and the ratio between Ohnishi Parameter. The ratio between experimental etching rates indicates that PMMA is 1.45 times more susceptible to etching than ZEP520A, and this susceptibility is smaller by 18% than 1.77, which is the susceptibility predicted by Ohnishi Parameters. Thus, since the experimental susceptibility is in good agreement with that predicted by Ohnishi Parameters, ZEP520A has been chosen. After the 2^{nd} RIE, as shown in FIG. 2, the features identical to the CAD layout were observed.

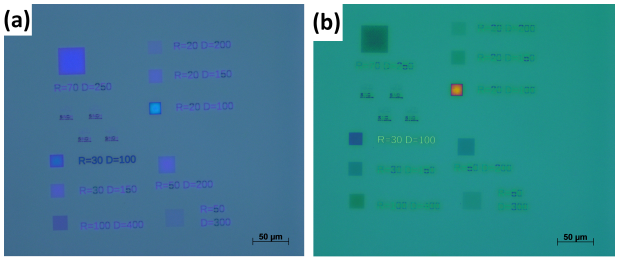

FIG. 2: (a) Optical microscope image of the patterns after development; (b) Optical microscope image of the patterns after 2^{nd} etching.

B. KOH etching

During KOH etching, the wafer will float up. Simultaneously, the reaction generates hydrogen gas, which forms a bubble layer and slows down the etching rate significantly. Therefore, it is necessary to immerse the wafer into the solution by an external force. The etching rate is estimated to be 1.2 µm/min. As shown in FIG.3, the 4 hours' etching resulted in the etching depth of 297.245 µm, which was measured by Zygo NewView 7300 Optical Profilometer. The etching depth can also be calculated to be 303.655 µm using the rule of the interplanar angle 54.7° and the window sizes of side 1 and 2 of 755 and 325 µm, respectively. The relative error is -2.11%, which indicates this etching depth estimation obtained by the optical microscope is a reliable and convenient method.

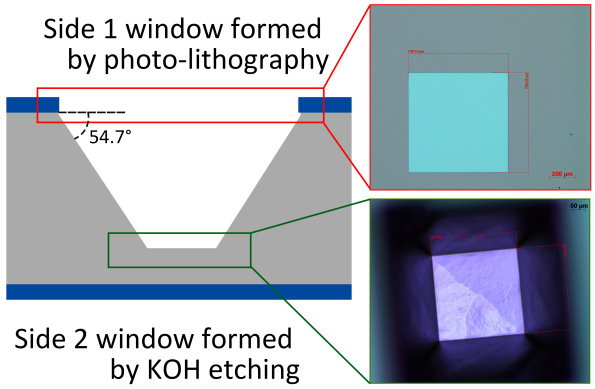

FIG. 3: Illustration of KOH etching after 4 hours, windows captured by optical microscope.

C. Fabrication of nanopore arrays

Since the window could not be observed through the other side, the position of the center of the chip needed to be calculated from the four vertices through the TV mode of Elionix e-beam writer to engrave the nanopore pattern at the right place. FIG. 4 shows SEM images of a series of nanopore structures using JEOL 7500F HRSEM. A diameter d of these nanopores ranges from 40 nm to 200 nm, whereas a center-to-center distance D is changes from 100 to 400 nm.

FIG. 4(a) shows that the resist film was completely broken under the condition of the 40 nm diameter nanopores with D = 100 nm (the edge-to-edge distance = 60 nm). FIG. 4(b), 4(d), and 4(e) indicate that the 40, 60, and 100 nm diameter nanopores with D = 150 and 200 nm (the edge-to-edge distance = 110 and 100 nm) are clearly observed, although their locations are irregularly displaced. FIG. 4(c) exhibits that the 60 nm diameter nanopore pattern with D = 100 nm (the edge-to-edge distance = 40 nm) turns into the "cellular" structure, which indicates the overdose. FIG. 4(g) also shows the displacement of nanopore location (d = 140 nm, D = 250 nm, and the edge-to-edge distance = 110 nm). On the other hand, FIG. 4(f) and 4(h) with the edge-to-edge distance = 200 nm show that the displacement of nanopore location and the "cellular" structure are not observed. The SEM results reveal that the displacement and the "cellular" structure of the nanopores should be ascribed to the proximity effect, which is an overdose effect due to e-beam back scattering in the silicon nitride layer. When the edge-to-edge distance is smaller than 110 nm, the experimental results indicate that the proximity effect becomes seriously.

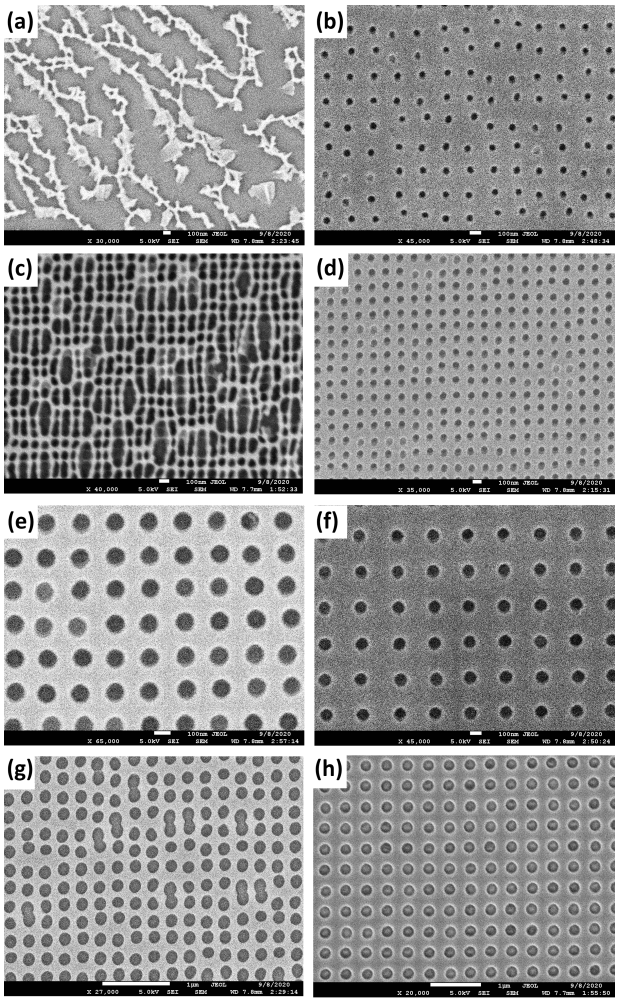

FIG. 4: SEM images of nanopore arrays with diameter d and center-to-center distance D. (a) $d = 40$ nm, $D = 100$ nm; (b) $d = 40$ nm, $D = 150$ nm; (c) $d = 60$ nm, $D = 100$ nm; (d) $d = 60$ nm, $D = 150$ nm, (e) $d = 100$ nm, $D = 200$ nm; (f) $d = 100$ nm, $D = 300$ nm; (g) $d = 140$ nm, $D = 250$ nm; (h) $d = 200$ nm, $D = 400$ nm.

IV. Summary

In conclusion, the fabrication method of making nanopore arrays on the free-standing silicon nitride with the desired feature size *via* EBL was successful. During the fabrication process, the reactive ion etching rate of SF_6 for silicon nitride and silicon has been achieved as 0.844 nm/s and 6.52 nm/s, respectively; the KOH etching rate for silicon is 1.2 µm/min at 75 °C. It was also proven that ZEP520A was a better resist towards reactive ion etching compare to PMMA due to its higher resistance towards etching and was corroborated theoretically by Ohnishi parameters obtained from each polymer's monomer. The minimum pore size of 40 nm was attainable by using EBL when the edge-to-edge distance between nanopores is 200 nm. The next step will focus on adjusting the size of the processed nanopore by atomic layer depostion and removing the residual silicon substrate under silicon nitride through xenon difluoride etching.

V. Acknowledgements

This work was performed at the Singh Center for Nanotechnology at the University of Pennsylvania, a member of the National Nanotechnology Coordinated Infrastructure (NNCI) network, which is supported by the National Science Foundation (Grant NNCI-2025608).

[1] Fan Xia Ruixue Duan and Lei Jiang. Constructing tunable nanopores and their application in drug delivery. *ACS Nano*, 7(10):8344–8349, 2013.

[2] Stephen Y. Chou and Wei Ding. Ultrathin, high-efficiency, broadband, omni-acceptance, organic solar cells enhanced by plasmonic cavity with subwavelength hole array. *Optics Express*, 21(S1):A60–A76, 2013.

[3] Andras Kis Ke Liu, Jiandong Feng and Aleksandra Radenovic. Atomically thin molybdenum disulfide nanopores with high sensitivity for dna translocation. *ACS Nano*, 8(3):2504–2511, 2014.

[4] Ariel J. Ben-Sasson and Nir Tessler. Unraveling the physics of vertical organic field effect transistors through nanoscale engineering of a self-assembled transparent electrode. *Nano Letters*, 12(9):4729–4733, 2012.

[5] Autumn T. Carlsen Martin Huber Furat Sawafta, Bason Clancy and Adam R. Hall. Solid-state nanopores and nanopore arrays optimized for optical detection. *Nanoscale*, 6:6991–6996, 2014.

[6] Ulrich F. Keyser. Enhancing nanopore sensing with dna nanotechnology. *Nature Nanotechnology*, 11:106–10, 2016.

[7] Hiromichi Yamamoto Unnati Joshi, Vishal Venkatesh. Progress report i: Fabrication of nanopores in silicon nitride membranes using self-assembly of ps-b-pmma, 2019. `https://repository.upenn.edu/scn_protocols/56/`.

[8] Hiromichi Yamamoto Kodai Watanabe, Unnati Joshi. Progress report i: Fabrication of nanopores in silicon nitride membranes using self-assembly of ps-b-pmma, 2019. `https://repository.upenn.edu/scn_protocols/61/`.

[9] Gerald G. Lopez and Glen de Villafranca. Discharge: Spin-on anti-charging agent for electron beam lithography, 2018. `https://repository.upenn.edu/scn_protocols/50/`.

[10] Meredith Metzler. Reactive ion etch (rie) of silicon nitride (sinx) with tetrafluoromethane (cf4), 2016. `https://repository.upenn.edu/scn_tooldata/37/`.

[11] S. Esho H. Gokan and Y. Ohnishi. Dry etch resistance of organic materials. *Journal of The Electrochemical Society*, 130(1):143, 1983.